

Research on 64-QAM subcarrier modulation for optical wireless communication

Ke Xizheng, Xie Mengqi, Shi Biyao

(School of Automation and Information, Xi'an University of Technology, Xi'an 710048, China)

Abstract: High-order Quadrature Amplitude Modulation (QAM) in a limited bandwidth can transmit more information than either BPSK or QPSK system. Therefore, the technology is widely used in cable communication systems. While optical scintillation affected the high-order QAM system easily. The multi-mode blind signal equalization is used to reduce the influence of scintillation caused by atmospheric turbulence. In simulation, the turbulence channel was modeled by Gamma-Gamma distribution. The constellation of receiving signal shows the different points dispersions under different channel noise situations. Results show that the transmitted signal was primarily affected by multiplicative noise. A 64-QAM experimental system is built to demonstrate the feasibility of the system under real situation.

Key words: 64-QAM; channel noise; constellation; free space optical communication; MMA equalizer

CLC number: TN929.1 **Document code:** A **DOI:** 10.3788/IRLA201847.S122003

无线光通信系统中 64-QAM 调制实验研究

柯熙政, 解孟其, 石碧瑶

(西安理工大学 自动化与信息工程学院, 陕西 西安 710048)

摘要: 高阶 QAM 较 BPSK/QPSK 能在有限的带宽内能传输更多的信息量, 因此广泛应于有线通信系统中。而对于无线光通信, 大气湍流引起的光强闪烁效应对高阶 QAM 信号的影响很大, 本文采用多模盲均衡算法克服此类噪声。系统仿真中使用 Gamma-Gamma 模型模拟大气湍流信道, 对比了不同噪声情况下接收信号星座图的聚敛性, 结果表明在传输过程中影响信号质量的主要因素是乘性噪声。最后搭建了 64-QAM 实验系统证明上述算法的可行性。

关键词: 64-QAM 调制解调; 信道噪声; 星座图; 自由空间光通信; MMA 均衡

收稿日期: 2018-03-05; 修订日期: 2018-05-03

基金项目: 国家自然科学基金(61377080); 国家科技创新基金(13C26213201867); 陕西省重点产业创新项目(2017ZDCXL-GY-06-01)

作者简介: 柯熙政(1962-), 男, 教授, 博士生导师, 博士, 主要从事无线光通信方面的研究。Email: xzke@263.net

0 Introduction

The advantages of optical wireless communication (OWC) are confidentiality, with strong anti-jamming capability, and low cost, and hence show great promise for transmission of voice image data. Many modulation methods have been applied, including OOK, PPM, and DPIM. Ghassemlooy et al. studied the bit-error-rate and power spectrum of digital pulse interval modulation for OWC^[1]. Mahdiraji et al. compared the bit-error-rate of three modulation methods (OOK, PPM, and DPIM) using an OWC system^[2], and showed that PPM has better error control capabilities. Hassan Zoheb et al. studied subcarrier modulation and quadrature amplitude modulation (QAM)^[3], and analyzed the system performance using negative exponential and K – distribution models. Ansari I S et al. analyzed the outage probability of RoFSO system under Gamma-Gamma channel model, which is a more universal model to describe the atmospheric turbulence channel^[4]. Vellakudiyan J. et al. investigated FSO system performance like bit error rate(BER), channel capacity and outage probability over a generic propagation model called M–distributed channel in the presence of atmospheric turbulence^[5]. High-order QAM is attractive for its high power utilization, strong anti-interference capability, and inclusion of more information on the limited bandwidth, so the fiber and FSO system attempt to apply high-order QAM^[6-7]. However, QAM transmission is affected by atmospheric turbulence, which increases inter-symbol interference and system bit-error-rate, causing significant difficulty for receiver detection, and there has been much research to address this problem.

Karaogus et al. presented a soft decision directed algorithm (SDD) suitable for QAM^[8]. The algorithm input signal constellation is a uniform block, but the block increases the complexity and instability of the algorithm, and slow convergence and easy to diverge. Miranda et al. proposed a dual mode constant modulus algorithm (DM–CMA)^[9], which combined

the calculation of the error term regional decision factor, effectively reducing the algorithm divergence. However, due to an error in the CMA model, non-constant modulus signals do not match, producing greater equilibrium steady state error in higher order QAM signals. Yang et al. proposed a multi-mode algorithm (MMA)^[10]. However, the computational complexity of the algorithm is high, and for higher order QAM to converge quickly, it is necessary to eliminate inter-symbol interference so the interference phase rotation can be corrected. Y. Wang et al. used a modified cascaded MMA for a visible light communication system^[11], and showed MMA can be used for OWC systems.

Here in this work, the multi-mode algorithm blind equalization has employed in 64–QAM FSO subcarrier modulation system to reduce the negative influence of atmospheric turbulence. Both simulation and short range experiment have been taken. The constellation diagrams in receiver show the effects of atmospheric turbulence, and the results are analyzed and discussed.

1 64–QAM wireless optical communication system

Atmospheric laser communication systems use a laser carrier to transmit information from one point to another. Thus, light is received at the destination, and demodulated to recover the original message, as shown in Fig.1.

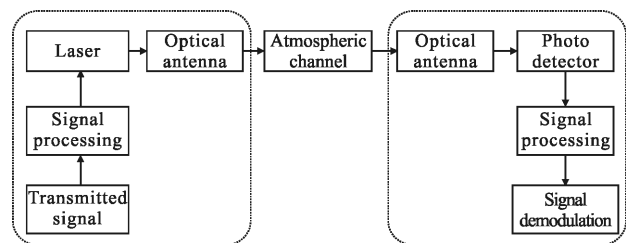


Fig.1 Block diagram of a wireless laser communication system

The signal processing module is used to modulate the signal. The processed signal is passed to the laser module and the electrical signal is converted to an

optical signal. The modulated optical signal is transmitted to the receiver through the optical telescope. After the propagation passed through the atmosphere, the optical signal is received by the optical telescope of the receiver module. And then the optical signal converts to an electrical signal by a photo detector (usually be a photodiode). Then the signal is demodulated, finally restore to the original information.

64-QAM uses both amplitude and phase of the carrier to transmit information. The modulation and demodulation scheme is shown in Fig.2. The signal is divided into in-phase(I) and quadrature (Q) signals. These signals can be composed 1 of 8 different levels. The combination of I and Q is mapped into a constellation points. Each constellation point represents 6-bit information. So there is $2^6=64$ kinds of different state.

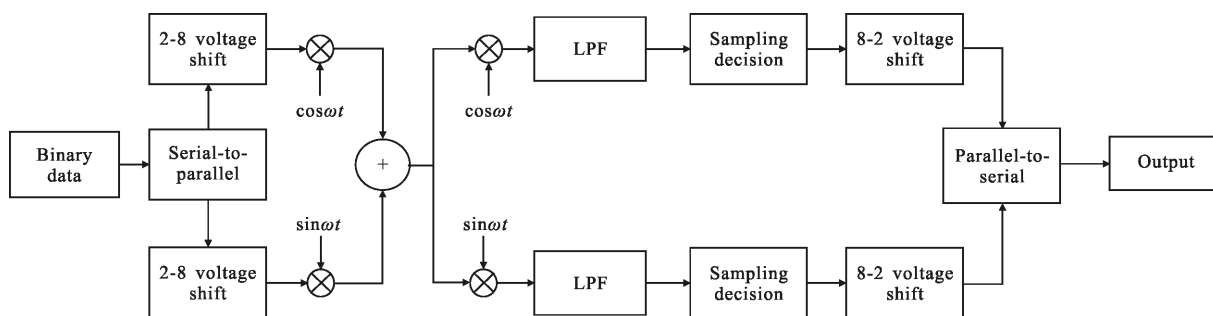


Fig.2 64-QAM Scheme

2 Multi-mode algorithm

Figure 3 shows the proposed equalization system. The input signal $s(n)$ experiences atmospheric turbulence channel $h(n)$, and additive Gaussian noise $v(n)$. Then multi-mode equalization is used to recover the signal $y(n)$.

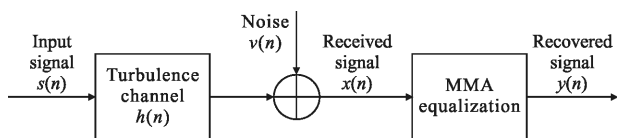


Fig.3 Multi-mode blind equalization model on atmospheric channel

Multi-mode blind equalization divides $y(n)$ into real and imaginary parts, $y(n)=y_R(n)+y_I(n)$. MMA cost function of the form of the following formula^[9]:

$$J_{\text{MMA}}=E\{[y_R^2(n)-R_R^2]\}+E\{[y_I^2(n)-R_I^2]\} \quad (1)$$

where $E[\cdot]$ is average, $R_R^2=E(a_n^4)/E(a_n^2)$, $R_I^2=E(b_n^4)/E(b_n^2)$. a_n and b_n are the real and imaginary parts of transmit signal $s(n)$. For QAM signal, $R_R^2=R_I^2=\gamma$. γ is called reference signal.

The error function is as follows:

$$e_{\text{MMA}}(n)=y_R(n)\{\gamma-y_R^2(n)\}+j\cdot y_I(n)(\gamma-y_I^2(n)) \quad (2)$$

The equalization filter $W(n)$ updates by the error

function $e_{\text{MMA}}(n)$ and the input signal with noise $X(n)$.

$$W(n+1)=W(n)+\mu\cdot e_{\text{MMA}}(n)\cdot X^*(n) \quad (3)$$

where μ is iterative steps.

3 Mixed noises channel model

To study the performance of 64-QAM system, we must first define the noise model, as shown in Fig.4.

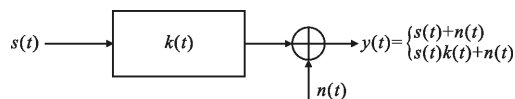


Fig.4 Noise model

Assuming the signal is $s(t)$, noise is $n(t)$, if receiving signal $y(t)$ is $s(t)+n(t)$, called $n(t)$ is additive noise. If receiving signal $y(t)$ is $s(t)k(t)+n(t)$, $k(t)$ is multiplicative noise.

Additive noise $n(t)$ is superimposed on the signal. whether or not there is a signal, $n(t)$ is always there. Additive white Gaussian noise (AWGN) is the most basic noise and interference model, with Gaussian amplitude distribution, and uniform power spectral density.

Multiplicative noise is only present when there is an underlying signal. If the signal disappears, the noise disappears. Gamma-Gamma model signal is

used as the multiplicative model.

We model the intensity distribution for Gamma-Gamma factorization as a product of two independent random processes, each containing a Gamma probability density function^[12]:

$$f_I(I) = \frac{2(\alpha\beta)^{(\alpha+\beta)/2}}{\Gamma(\alpha)\Gamma(\beta)} \cdot I^{(\alpha+\beta)/2-1} \cdot K_{\alpha-\beta}(2\sqrt{\alpha\beta I}), I>0 \quad (4)$$

where I is the optical signal strength, α and β are the probability density function parameters, $\Gamma(\cdot)$ is the Gamma function, and $K_{\alpha-\beta}(\cdot)$ is the modified Bessel function of the second kind with $\alpha-\beta$ order.

For a simple condition of atmospheric turbulence, α and β are related to σ_R^2 . The σ_R^2 is called Rytov variance, which is the logarithmic light intensity fluctuation variance. So σ_R^2 is used to characterize atmospheric turbulence intensity.

$$\begin{cases} \alpha = \left(\exp\left(\frac{0.49\sigma_R^2}{(1+1.11\sigma_R^{12/5})^{7/6}}\right) - 1 \right)^{-1} \\ \beta = \left(\exp\left(\frac{0.51\sigma_R^2}{(1+0.69\sigma_R^{12/5})^{5/6}}\right) - 1 \right)^{-1} \end{cases} \quad (5)$$

Transmission performance is discussed below for different values of σ_R^2 . We also discuss the effect of noises on the 64-QAM signal for two cases: (1) Impact of receiving signal constellation in Gamma-Gamma channel under multiplicative noise only; (2) Impact of receiving signal constellation in Gamma-Gamma channel under both multiplicative and additive noises.

4 Results

The simulation model corresponding to Fig.2 was investigated for additive and multiplicative noise.

The 64-QAM modulated signal is subject to Gamma-Gamma noise distribution from atmospheric interference, i.e., multiplicative noise, and the sender constellation is shown in Fig.5. In the case of weak turbulence, $\sigma_R^2=0.05$, the received 64-QAM constellation is shown in Fig.6. Figure 7 shows the raw received constellation for $\sigma_R^2=0.3$ without MMA. Figure 8 shows the MMA results of the received constellation for the same σ_R^2 .

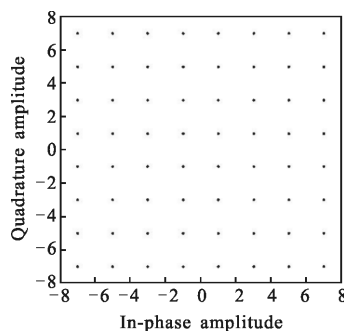


Fig.5 Modulation signal constellation

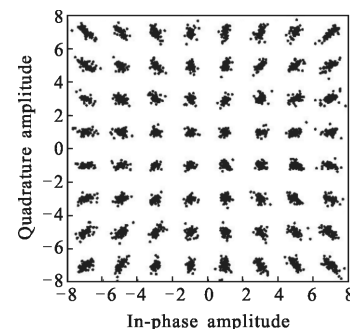


Fig.6 64-QAM demodulation constellation under weak turbulence ($\sigma_R^2=0.05$)

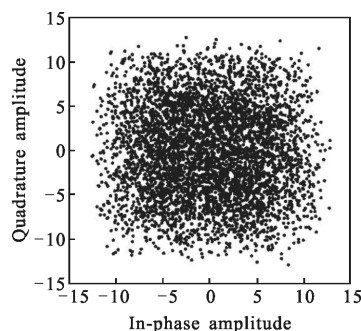


Fig.7 64-QAM demodulation constellation under strong turbulence ($\sigma_R^2=0.3$) without MMA

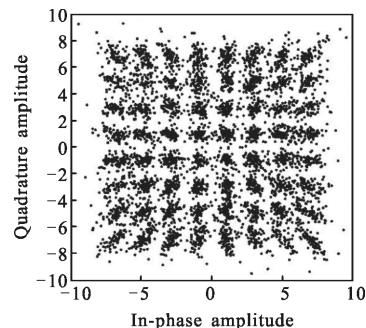


Fig.8 MMA processed 64-QAM demodulation constellation under strong turbulence ($\sigma_R^2=0.3$)

The horizontal axis is the I signal level, and the vertical axis is the Q signal level. Both coordinates

are dimensionless. Without noise affects, the constellation diagram consists of 64 points. In weak turbulence condition, Fig.6 shows the constellation points are almost clear with a little dispersion. The multiplicative noise has very big impact on the receiving constellation. In Fig.7, the receiving constellations become chaotic because the σ_R^2 rises to 0.3. MMA equalization is employed to solve this problem. The result shows that multiplicative noise causes the radial diffusion of the constellation points.

4.1 Mixed noise

Under weak turbulence we consider joint noise impact. Figure 9 shows the received 64-QAM constellation for additive noise signal-to-noise ratio (SNR)=15, $\sigma_R^2=0.1$. Figure 10 shows the case of SNR=10, $\sigma_R^2=0.1$. And Fig.11 shows the case of SNR=10, $\sigma_R^2=0.3$. All these results are processed by MMA equalization.

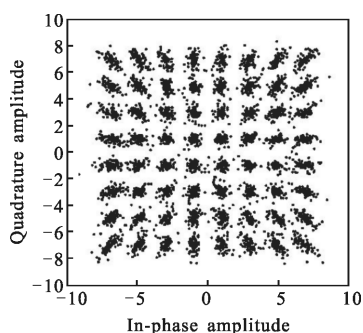


Fig.9 Demodulated received constellation with SNR=15, $\sigma_R^2=0.1$

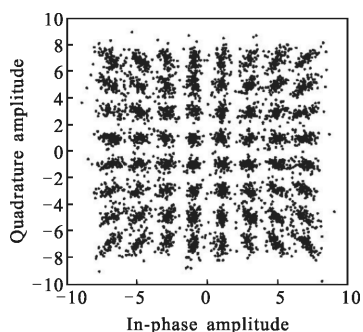


Fig.10 Demodulated received constellation with SNR=10, $\sigma_R^2=0.1$

When the SNR of additive noise is fixed at 10 dB, the constellation dispersion increased with turbulence intensity increasing. When the turbulence intensity is fixed at 0.1, there is little change in the constellation

with increasing SNR from 15 dB to 10 dB. Therefore, while both noise types affect the 64-QAM system during transmission, multiplicative noise is the major factor.

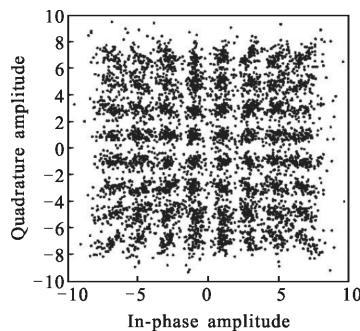


Fig.11 Demodulated received constellation with SNR=10, $\sigma_R^2=0.3$

4.2 BER analyses

Table 1 and Fig.12 show the BER results of the system under different SNR and turbulence intensities.

Tab.1 BER for different SNR and turbulence intensities

Multi- plicative noise	Additive noise					
	SNR=20 dB	SNR=18 dB	SNR=16 dB	SNR=14 dB	SNR=12 dB	SNR=10 dB
$\sigma_R^2=0.01$	0.0083	0.0256	0.0509	0.0820	0.1137	0.1532
$\sigma_R^2=0.05$	0.0146	0.0304	0.0543	0.0842	0.1173	0.1548
$\sigma_R^2=0.3$	0.1079	0.1175	0.1311	0.1478	0.1675	0.1928
$\sigma_R^2=1$	0.2549	0.2586	0.2625	0.2697	0.2768	0.2888

For relatively large SNR and weak turbulence situation, the BER of the system is very low. As SNR decreases or turbulence intensity increases, the BER is increased rapidly.

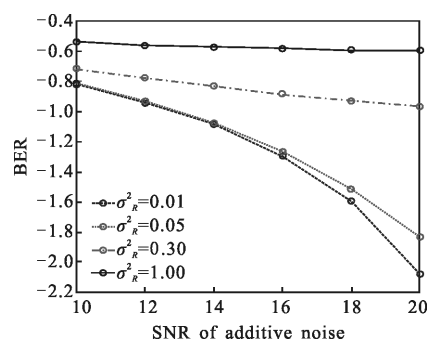


Fig.12 BER performance with different noise levels

4.3 Experiment results

The experiment instruments which include FPGA, DAC and analog lasers etc. are described in Ref.[13]. Experiments are performed to simulate atmospheric interference on the 64-QAM signals, as shown in Fig.13. When the transmission distance is relative close (<100 m), the constellation points show a little additive noise interference. And the radial diffusions caused by multiplicative noise are very clear at the edge of the constellation.

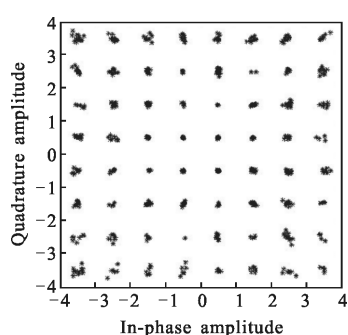


Fig.13 Receiver and transmitter constellations

5 Conclusion

A signal model is devised based on 64-QAM subcarrier modulation OWC systems, incorporating multi-mode equalization to improve performance. Gamma-Gamma distributed multiplicative and additive Gaussian noise is introduced to simulate intensity fluctuation and electric background noise in transmission. And explore the influence of different noises on constellation. The proposed model is primarily affected by multiplicative noise, which causes radial diffusion, especially on the edge of constellation diagram.

References:

[1] Ghassemlooy Z, Hayes A R, Seed N L. Digital pulse interval modulation for optical communications [J]. *IEEE Communication Magazine*, 1998, 36(12): 95-99.
 [2] Chafour Amouzad Mahdiraji, Edmond Zahedi. Comparison of selected digital modulation schemes (OOK, PPM and DPIM)

for wireless optical communications [C]//4th Student Conference on Research and Development, 2006, 27-28: 5-10.
 [3] Md. Zoheb Hassan, Song Xuegui, Cheng Julian. Subcarrier intensity modulated wireless optical communications with rectangular QAM [J]. *Journal of Optical Communications and Networking*, 2012, 4(6): 522-532.
 [4] Ansari I S, Abdallah M M, Alouini M S, et al. Outage performance analysis of underlay cognitive RF and FSO wireless channels [C]//3rd International Workshop in Optical Wireless Communications IEEE, 2014: 6-10.
 [5] Vellakudiyani J, Muthuchidambaramanathan P, Bui F M, et al. Performance of a subcarrier intensity modulated differential phase-shift keying over generalized turbulence channel[J]. *AEU-International Journal of Electronics and Communications*, 2015, 69(11): 1569-1573.
 [6] Tang J, He J, Li D, et al. 64/128-QAM half-cycle subcarrier modulation for short-reach optical communications [J]. *Photonics Technology Letters IEEE*, 2015, 27(3): 284-287.
 [7] Rakesh V S, Singhal R. 720-Mbps 64-QAM-OFDM SCM transmission over RGB-LED-based FSO communication system [C]//13th International Conference on Wireless and Optical Communications Networks, 2016: 1-5.
 [8] Karaogus J, Arallan S H. A soft decision-directed blind equalization algorithm applied to equalization of mobile communication channels[C]//ICC, 1992, 343(4): 41-45.
 [9] Miranda M D, Silva M T M, Nascimento V H. Avoiding divergence in the constant modulus algorithm[C]//Acoustics, Speech, and Signal Processing, IEEE International Conference, 2008: 3565-3568.
 [10] Yang J, Werner J J, Dumont G A. The multimodulus blind equalization and its generalized algorithms[J]. *IEEE Journal on Selected Areas in Communications*, 2002, 20(5): 997-1015.
 [11] Wang Y, Tao L, Huang X, et al. Enhanced performance of a high-speed WDM CAP64 VLC system employing Volterra series-based nonlinear equalizer[J]. *IEEE Photonics Journal*, 2015, 7(3): 1-7.
 [12] Andrews L C, Philips R N. Laser Beam Propagation through Random Media [M]. 2nd ed. Bellingham, Washington, USA: SPIE Press, 2005.
 [13] Xie Mengqi, Ke Xizheng. Cyclic spectral density analysis of free space optical sub-carrier signals [J]. *Acta Optica Sinica*, 2015, 35(2): 0201001. (in Chinese)